Thermally induced orientational flipping of cylindrical phase diblock copolymers

ARTICLE *in* JOURNAL OF MATERIALS CHEMISTRY C · JANUARY 2014

Impact Factor: 4.7 · DOI: 10.1039/C3TC32283A

Journal of Materials Chemistry C

PAPER

View Article Online
View Journal | View Issue

Thermally induced orientational flipping of cylindrical phase diblock copolymers†

Cite this: J. Mater. Chem. C, 2014, 2, 2175

F. Ferrarese Lupi,[a] T. J. Giammaria,[ab] G. Seguini,[a] M. Laus,*[b] E. Enrico,[c] N. De Leo,[c] L. Boarino,[c] C. K. Ober[d] and M. Perego*[a]

Received 19th November 2013
Accepted 4th January 2014

DOI: 10.1039/c3tc32283a

www.rsc.org/MaterialsC

Cylinder forming PS-*b*-PMMA block copolymer (BCP) thin films were deposited on pre-patterned surfaces with densely packed and nanometer wide trenches defined by conventional top down approaches and arranged to form a periodic grating. The films were subsequently annealed at 250 °C for times ranging from 30 s to 900 s in a rapid thermal processing device and their morphology evolution within the topographically defined structures was systematically investigated. Irrespective of the surface neutralization, an irreversible orientational flipping of the BCP microdomains inside the trenches was observed and attributed to de-swelling of the polymeric film as a consequence of a progressive desorption of the solvent retained inside the film. Systematic investigation of the annealing process indicates that the flipping is strongly dependent on the geometric parameters of the trenches and on the relative position of the analysed trench with respect to the periodic topographic structure.

Introduction

With no technology solutions currently available to meet the requirements of the International Technology Roadmap for Semiconductors (ITRS) for manufacturing devices with feature sizes of 15 nm and below in 2016 (termed the 22 nm technology node), the use of self-assembling materials has emerged as a significant option for microelectronic patterning strategies.[1] The self-assembly on the scale of phase segregation of block copolymer (BCP) thin films has been largely investigated during the last 15 years and has become a mature field in polymer science.[2,3] By combining "bottom up" self-assembly of BCPs with "top-down" patterned templates, it is possible to register the periodic domains of the nanostructured film with the underlying topographically defined structure and to improve the long-range order of the nanostructures, thereby simultaneously reducing defect formation and increasing size uniformity.[4–8] The integration of these self-assembling materials with current 193 nm photolithographic techniques is expected to provide a viable and low cost solution to fabricate sub-lithographic features and to overcome the fundamental physical limitations of the current technology.

To be competitive with the high quality standards of traditional top-down approaches, the exploitation of the technology based on self-assembling materials for very-large-scale production by the semiconductor industry requires absolute control of the process. In this respect, the study of the BCP evolution inside periodic topographical structures is of great significance since in any real microelectronic device, the pre-patterned structures that must be filled with BCPs are not expected to be isolated and proximity effects and crosstalk among neighboring structures should be accounted for.[9–12] Consequently, a deep understanding of the intimate mechanisms driving the self-assembly process on pre-patterned substrates is required to reduce the film defectivity and optimize the processing time.

Usually, the organization of a block copolymer microdomain is promoted by annealing the polymeric film at a temperature well above the glass transition[13,14] or by plasticizing the BCP *via* exposure to solvent vapours.[15,16] In particular, Solvent Vapour Annealing (SVA) has been extensively studied due to the possibility of reducing the self-assembly time inside periodic topographic structures from days to a few minutes.[17] In spite of the significant interest that such techniques stimulated, poor understanding of the mechanism governing the SVA process and the absence of a standardized method prevent its present exploitation for large-scale production. Indeed, the SVA technique requires a high degree of control of all the parameters involved in sample preparation, such as the annealing temperature, size of annealing chamber, proximity of the sample to the liquid surface, purity of the solvent and leak rate.

[a]*Laboratorio MDM, IMM-CNR, Via C. Olivetti 2, 20864 Agrate Brianza, MB, Italy. E-mail: michele.perego@mdm.imm.cnr.it; Fax: +39 039 6881175; Tel: +39 039 6036383*

[b]*Dipartimento di Scienze e Innovazione Tecnologica (DISIT), Università del Piemonte Orientale "A. Avogadro", INSTM, UdR Alessandria, Viale T. Michel 11, 1512 Alessandria, Italy. E-mail: michele.laus@mfn.unipmn.it*

[c]*NanoFacility Piemonte, Istituto Nazionale Ricerca Metrologica, Strada delle Cacce 91, 10135 Torino, Italy*

[d]*Department of Materials Science and Engineering, Cornell University, Bard Hall, Ithaca, New York 14853, USA*

† Electronic supplementary information (ESI) available. See DOI: 10.1039/c3tc32283a

Moreover, the environmental conditions of the laboratory in which the SVA process is performed (*i.e.* relative humidity) could adversely affect the reproducibility of the process.[18]

In a recent report, the self-assembly of cylindrical polystyrene-*b*-methylmethacrylate (PS-*b*-PMMA) structures oriented perpendicular with respect to a silicon substrate that was neutralized with end-grafted polystyrene-*r*-methylmethacrylate P(S-*r*-MMA) random copolymer (RCP) brushes was obtained on a flat surface in as few as 10 s using the Rapid Thermal Processing (RTP) technique.[19] This new self-assembly process presents several advantages compared to conventional thermal treatment since a direct and extremely fast modulation of the temperature is possible by properly tuning the power of the radiation sources used to heat the sample. In addition, this technology does not require the assistance of a solvent, apart from that naturally entrapped in the polymeric film after the spinning process, thus allowing RTP to be easily integrated into a standard lithographic workflow.

In the present work, the RTP technology is employed to elucidate the dynamics of BCP ordering within pre-patterned topographic structures with densely packed and nanometer wide trenches defined by conventional top down approaches and arranged to form periodic gratings. The in-plane geometrical parameters characterizing these structures (*i.e.* trench width W and distance d between two adjacent trenches) were selected taking into account the issue of commensurability between the topographic structure and the natural lattice spacing of the asymmetric PS-*b*-PMMA BCP.[20,21] A detailed and systematic investigation of the dynamics of BCP ordering is proposed as a function of the in-plane geometric parameters and processing conditions. These experimental findings delineate a clear picture of the driving forces directing the ordering process of the BCP microdomains within topographically defined structures during the RTP treatment.

Results and discussion

Orientational flipping phenomena in topographically confined BCP thin films

Periodic topographic structures, consisting of ten trenches placed side by side to form a periodic grating, were fabricated by e-beam lithography. The geometric parameters characterizing these structures are illustrated in Fig. 1a, where d represents the distance between the pre-patterned structures and W and t are the trench width and depth, respectively. To look into the effect of the nature of the trench surface on the dynamics of the cylindrical microdomain organization, two series of experiments were performed. In the first series, the BCP film was deposited on the silicon surface neutralized with a hydroxy-terminated P(S-*r*-MMA) RCP schematically depicted by the red layer in Fig. 1b. The grafted RCP layer guarantees a non-preferential interaction of the two blocks with the substrate. A second series of samples was then prepared by spinning the BPC directly onto the bare SiO_2 (Fig. 1c) without any previous surface treatment.

The grafting of the P(S-*r*-MMA) random copolymer on the pre-patterned SiO_2 substrate was performed *via* RTP treatment at 250 °C for 300 s. As the asymmetric PS-*b*-PMMA with a molecular mass of 67 kg mol^{-1} was used, the P(S-*r*-MMA) with a styrene fraction of 0.62 and M_n = 13.5 kg mol^{-1} was employed to neutralize the surface.[19] The non-grafted chains were then removed by sonication in toluene, resulting in a ~7.8 nm thick brush layer, measured by ellipsometry on the flat portion of the substrate, far away from the periodic structures. Such a value of thickness lies well inside the thickness window that is suitable to promote the perpendicular orientation of the nano-domains with respect to the substrate. For both neutralized and non-neutralized substrates, the spin-coating parameters for the BCP deposition were adjusted to supply a 28 nm thick polymeric film. The subsequent annealing process was performed by RTP

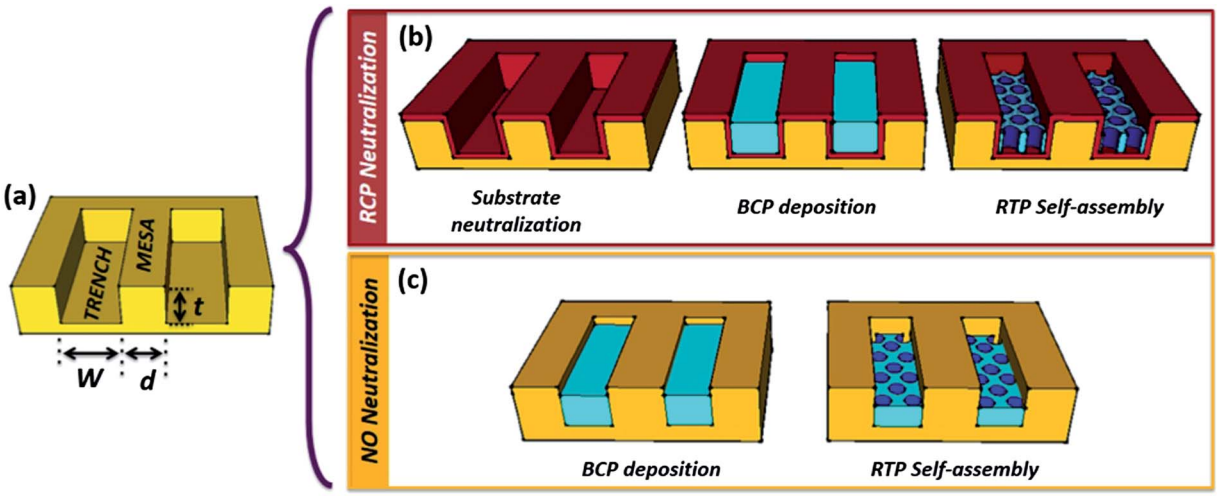

Fig. 1 Scheme of the periodic topographic structures (a). RTP preparation with substrate neutralization using a RCP (b) or onto the bare SiO_2 (c). For both substrates, the deposition of the block copolymer was performed *via* spin-coating and the directed self-assembly of the BCP was promoted by RTP annealing at 250 °C.

heating the samples at 20 °C s^{-1} up to 250 °C and then annealing at this temperature for different time periods.

Fig. 2 reports the planar view of SEM images representing the BCP on the RCP functionalized substrates in the flat region far away from the gratings (Fig. 2a) and within the topographically defined structures (Fig. 2b–d) at different stages of the ordering process. On the flat surfaces, far away from the periodic structures, the RTP thermal treatment promoted a fast ordering of the nanometer-scale BCP film, in the timescale of few tens of seconds, forming well defined microdomains with perpendicularly oriented hexagonally packed cylinders, in perfect agreement with previous findings.[22] Conversely, a substantially different behaviour in terms of BCP organization was observed when the polymeric film was confined within the topographic structures. The SEM images of Fig. 2a and b indicate that opposite orientations of the microdomains with respect to the substrate were obtained outside and inside the trenches after a 60 s thermal treatment at 250 °C.

In the latter case, the PMMA cylinders are arranged parallel to the substrate and perpendicular to the trench long axis as highlighted in the close view reported in Fig. 2e. This result suggests that the directed self-assembly process inside the topographically defined structures is strongly dependent on the interfacial interactions between the sidewalls and the two blocks.[23] As the annealing time increases, a progressive evolution of the film morphology is observed, with a flipping of PMMA cylinders from a parallel to perpendicular orientation with respect to the substrate. After 300 s annealing at 250 °C, some islands of features oriented perpendicular to the substrate emerge (Fig. 2b) whereas after 900 s, the complete flipping of the orientation is achieved (Fig. 2d) in the entire 8 μm length of the trenches. Accordingly, the flipping mechanism appears to be that of nucleation and growth, in which islands featuring the perpendicular structure are observed to form, progressively grow and merge until a complete reorientation of the system is achieved (Fig. 2f).

Without any surface neutralization, the orientation of the cylinder morphology is expected to be parallel to the substrate, because of the selective interaction of the substrate with the PMMA.[24,25] Fig. 3 reports the planar view of SEM images representing the BCP deposited on the bare SiO_2 without any surface neutralization. On the flat unpatterned surface, the parallel orientation of the PMMA cylinders with respect to the substrate is obtained after RTP treatments at 250 °C, even for annealing times as short as 30 s (Fig. 3a). Longer annealing times do not induce any orientational reorganization but simply improve the lateral ordering thus increasing the correlation length of the system.[25] In contrast, inside the topographic structures, in the early stages of the ordering process at 250 °C (60 s annealing time, Fig. 3b), the cylinders are oriented parallel to the long axis of the trench. As the annealing time increases, a reorientation process is observed to occur involving the orientation flipping from the parallel to the perpendicular cylinder morphology. The flipping process starts from the edges of the trench and proceeds from both sides to the middle of the trench. After 300 s annealing time, some parallel cylinders in the middle of the trench are still visible (Fig. 3c) but disappear after 600 s annealing time (Fig. 3d).

Orientational flipping dynamics in topographically confined BCP thin films

Although the behaviour so far delineated is quite general, quantitative differences were observed depending on the

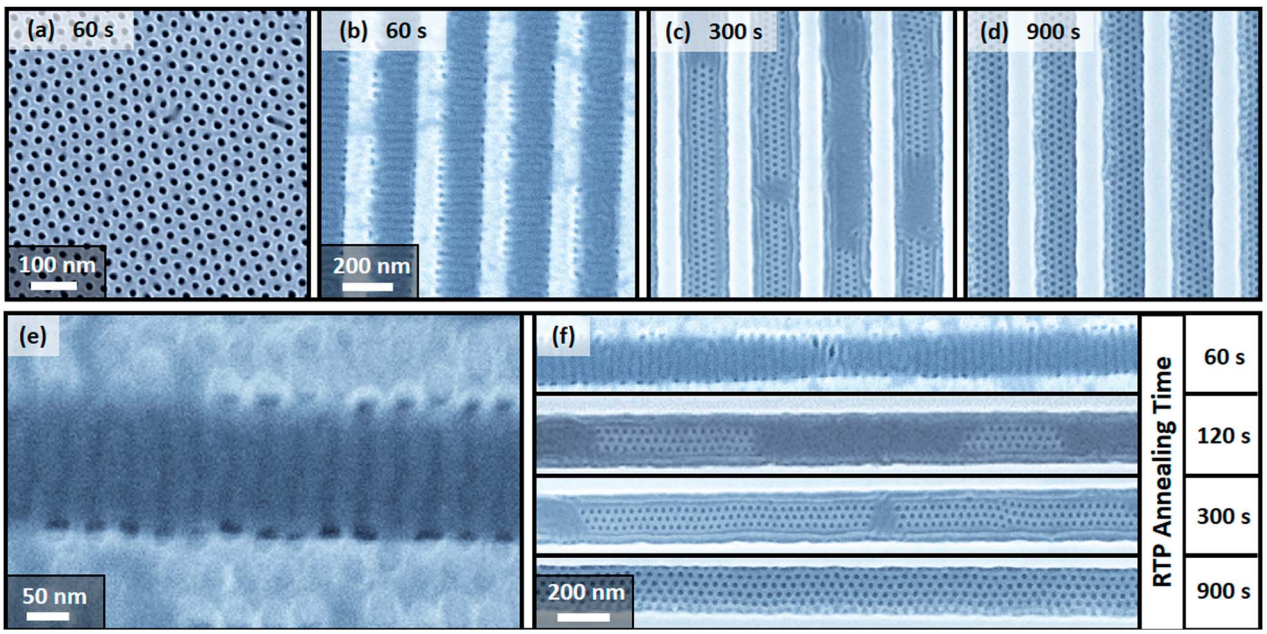

Fig. 2 RTP processing of the BCP on the flat surface (a) and inside the periodic topographic structure after annealing of 60 s (b), 300 s (c) and 900 s (d). (e) Magnified view of the 60 s annealed sample illustrating the presence of perpendicularly oriented cylinders across the trench edges. (f) Temporal evolution of the BCP indicating the nucleation and growth mechanism.

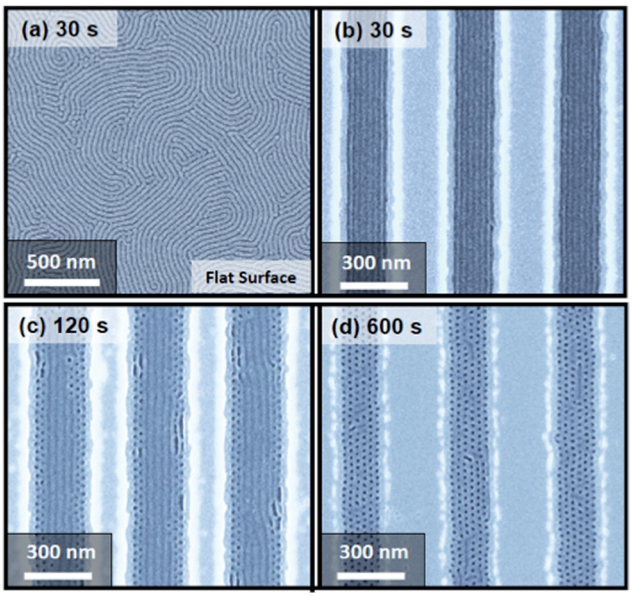

Fig. 3 SEM images illustrating the parallel orientation of the BCP on the flat not neutralized surface (a) and the morphological orientation evolution as a function of the annealing time inside the trenches (b)–(d).

specific geometric characteristics of the topographic structures and on the position of the trench within the grating. To delve into these aspects, the flipping propensity of the BCPs in periodic topographically defined structures consisting of ten trenches with W ranging from 120 to 210 nm and $d = 100$ nm or 200 nm was analyzed. This analysis was performed on the first set of samples with RCP functionalized surfaces. The fraction f of areas of perpendicular orientation with respect to the total area of the trenches constituting the grating is reported in Fig. 4 as a function of the annealing time for different values of trench width W (for $d = 100$ nm) and for different trench distances ($d =$ 100 nm and 200 nm). The flipping rate increases steadily as the trench width increases (Fig. 4a). Conversely, the flipping rate increases as the distance between two adjacent trenches decreases (Fig. 4b). This behavior is reproduced in all the grating irrespective of W (Fig. S1 in the ESI†).

The data reported in Fig. 4 refer to the overall behaviour of the entire grating consisting of ten trenches. However, substantial differences exist among the individual trenches, depending on their relative position in the grating, as illustrated in Fig. 5. The flipping rate decreases symmetrically on moving from the central trenches to the peripheral areas. In order to provide more insight into this process, the $f/2$ parameter (indicating the situation in which half of the total area inside the trenches is perpendicularly oriented) could be taken as an index to monitor the flipping kinetics. In the case of the two trenches in the middle of the grating $f/2$ is reached after about 100 s whereas, for the external trench, the time corresponding to $f/2$ is about 600 s (see Fig. 5b).

The same orientation flipping behaviour as a function of the geometric parameters was observed in the case of non-neutralized substrates as depicted in Fig. 6 representing a BCP thin film after RTP treatment at 250 °C for 120. The propensity

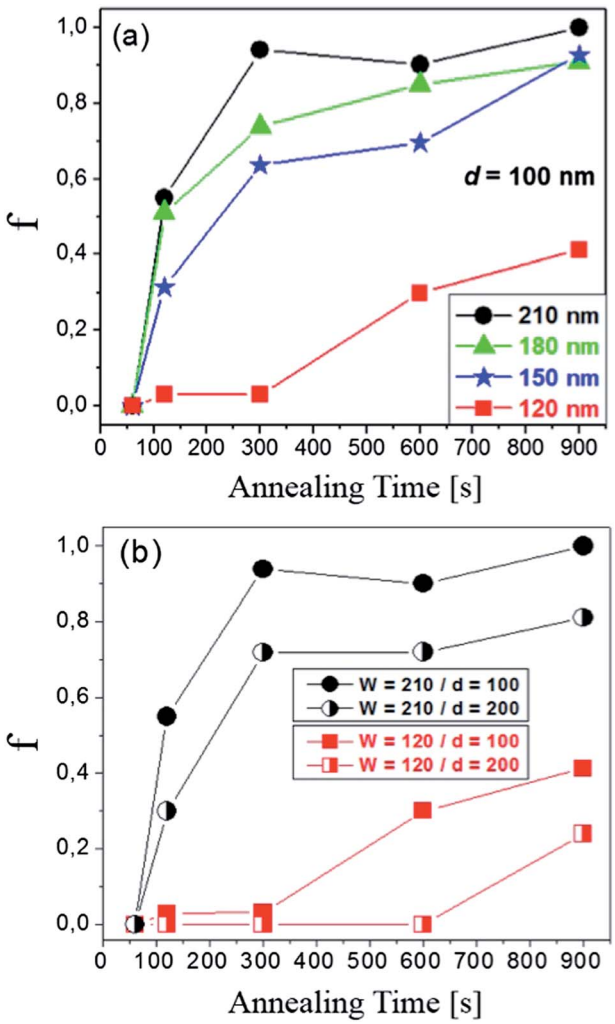

Fig. 4 Fraction of perpendicularly organized areas f as a function of the annealing time at 250 °C for different values of trench width W (for $d = 100$ nm) (a) and for different trench distances ($d = 100$ nm or 200 nm) (b). The error on the reported values is below 5%.

for flipping from the parallel orientation along the long axis of the trench to the perpendicular orientation depends on the position of the trench within the grating and decreases in moving from the central trenches to the peripheral ones. These data demonstrate that the BC self-assembly process in topographically defined structures is strongly influenced by the presence of other structures due to proximity effects. In addition, SEM data in Fig. 6 suggest the possibility to engineer the processing conditions in order to properly drive these phenomena. In principle, mixed morphologies with parallel cylinders in the central part of the trench and a well defined number of rows in which the cylinders are oriented perpendicular near the sidewalls can be employed to obtain adjacent dots and striped structures.

Discussion

The experimental results reported in the previous sections clearly demonstrate that the reorientation process dynamics of

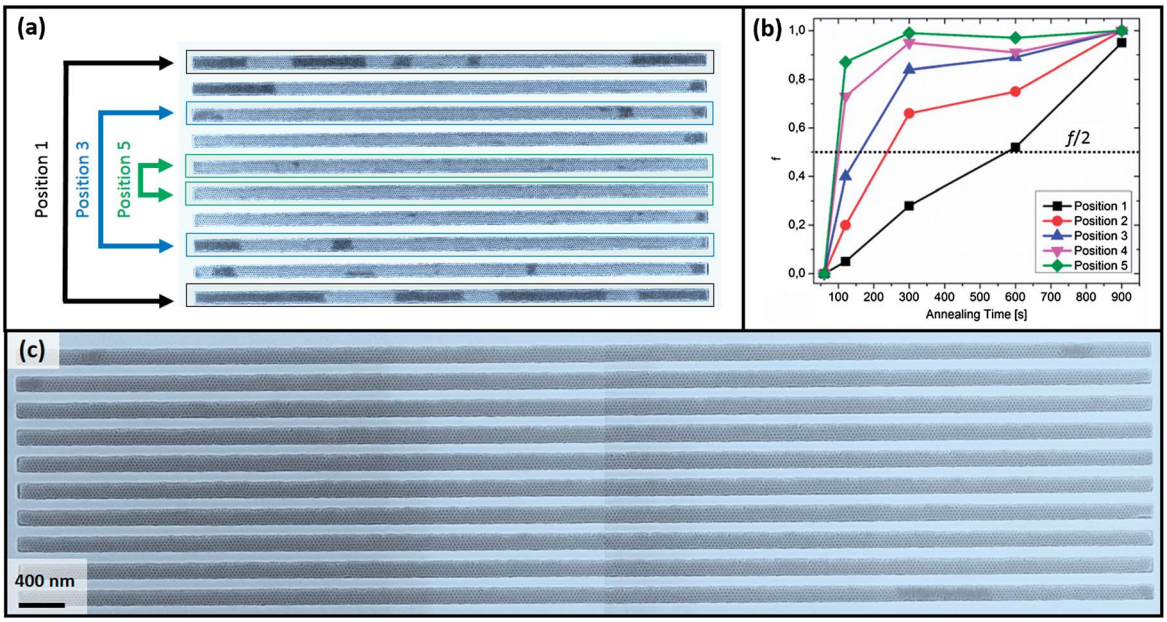

Fig. 5 (a) SEM image of the trench position in the grating. The dark zones consist of parallel oriented cylinders whereas in the light regions the orientation is perpendicular to the substrate. (b) Fraction of perpendicularly organized areas f as a function of the annealing time at 250 °C for the individual trenches with $W = 150$ nm and $d = 100$ nm. (c) Combined SEM images reporting the grating over the whole 8 μm length after annealing for 900 s.

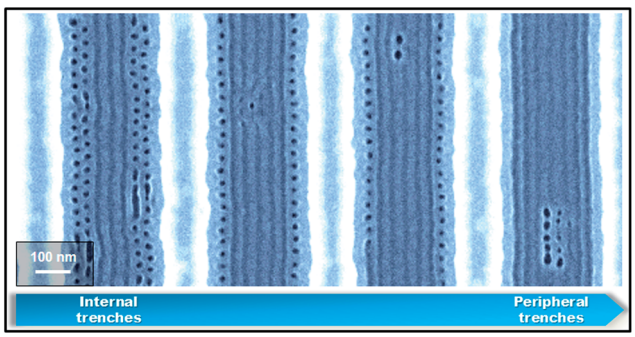

Fig. 6 Mixed morphologies consisting of parallel and perpendicular cylindrical features in successive trenches from the center (left) to the outer side (right) of the grating obtained by performing the RTP treatment for 120 s at 250 °C on the BCP film deposited over a non-neutralized patterned substrate.

the cylindrical morphology within the topographically defined structures depend on a number of variables and involve a complex mechanism. It is worth noting that the orientation flipping in the BCP nano-domains was observed by other authors in BCP films treated *via* solvent annealing.[26] The authors ascribed such an unexpected behaviour to a cyclical swelling and de-swelling mechanism of the nanometric polymeric film due to the variation of the solvent content inside the film. However, no evidence of flipping phenomena was reported so far in the case of conventional thermal treatments in a furnace or oven. To rationalize the data described so far we have to take into account the peculiar characteristics of RTP technology.

After BCP deposition, far from the grating, the surface of the film is perfectly flat but, in correspondence to the grating, the film should adopt a sinusoidal arrangement in order to account for the presence of the topographic structures.[27,28] When the film is heated up over the glass transition temperature, the mobility of the polymeric film increases and the capillarity forces allow the macromolecules to flow from the mesa into the trenches.[29,30] These phenomena were already reported to generate a relatively wide area surrounding the gratings not covered with the BCP, in the case of conventional annealing in a furnace.[31] In the present case, clear evidence of the flow of the BCP is provided by a comparison of the mesa structures for samples annealed at different times. In Fig. 2e the presence of a stretched BCP film, featuring cylinders with a shape elongated toward the flow direction (parallel to the substrate surface and perpendicular to the main axis of the trench) is apparent, whereas in Fig. 2d the mesas are completely clean.

According to this observation, during the flow stage, the film is likely to experience an elongational stress in the direction perpendicular to the main axis of the trench. This situation is tentatively sketched in Fig. 7a. The tensile stress derives from the release, during the RTP treatment, of the internal stresses generated by the spinning process and that frozen in the film when the glass transition of the system of BCP + solvent reaches room temperature and by the action of the capillary forces exerted on the film by the trenches themselves. The tensile stress is maximum in the middle of the grated zone and progressively reduces on going toward the periphery due to the progressive reduction of the lateral constraints acting on the film. The tensile stress produces a thinning of the film and ultimately leads to film fracture followed by a final flow of the

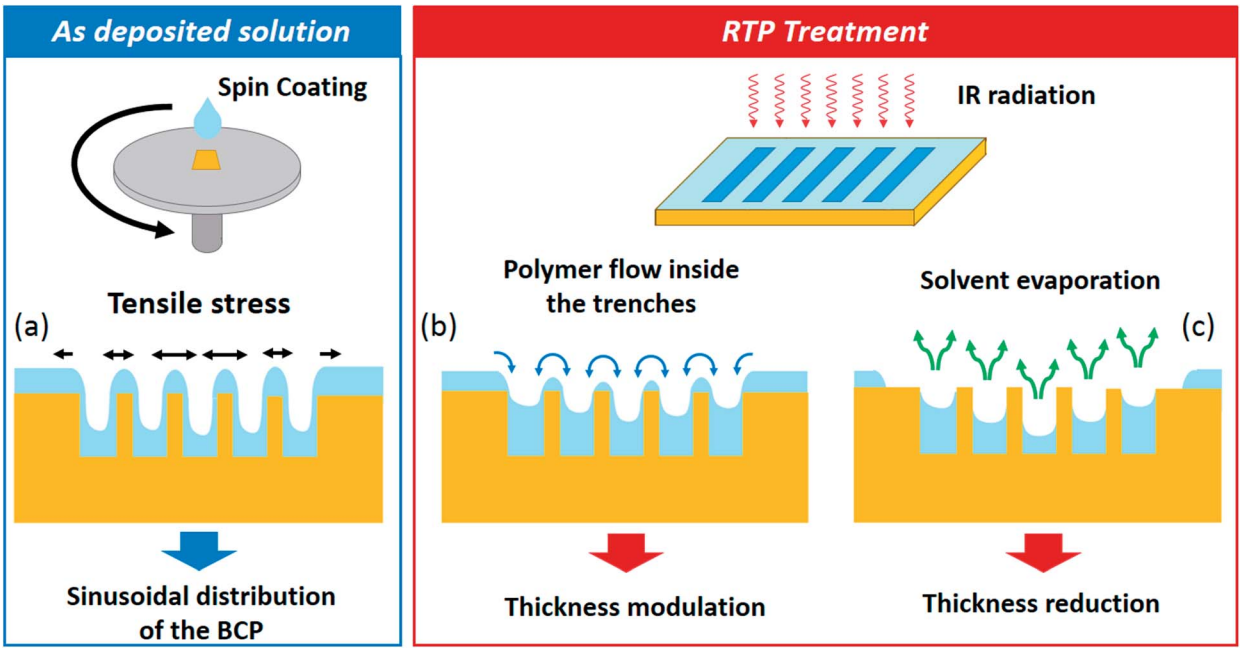

Fig. 7 (a) Sinusoidal distribution of the BCP on the periodic topographic structure, causing a variable tensile stress on the nanometric film. (b) Polymer flow inside the trenches as a consequence of the RTP annealing over the glass transition temperature. (c) Solvent evaporation during the RTP treatment results in a reduction of polymeric film inside the trenches.

block copolymer inside the trenches during the annealing process (see Fig. 7b). The observation that the central mesas are systematically cleaned faster than the peripheral ones is in perfect agreement with this mechanism. It is worth noting that the peripheral trenches have a larger polymer reservoir than the central trenches due to the very large extension of the surface they face outside the grating. As a consequence, the film thickness is minimum in the central trenches and increases progressively toward the periphery, as confirmed by cross-sectional SEM images on representative samples (Fig. S2, ESI†).

In addition, the amount of block copolymer in the trenches is strictly related to the amount of BCP available on the mesa: the larger the mesa, the larger the amount of polymer that flows into the trenches during the initial stage of the thermal treatment and, consequently, the thicker the polymeric film in the trenches. A similar reasoning applies for a fixed width of the mesa when decreasing the width of the trenches: the smaller the trenches, the thicker the polymeric film inside the trenches. In this context, it is important to keep in mind that even slight changes in the film thickness would have a dramatic effect on the structural orientation of the microdomains within thin films, since the perpendicular orientation can be achieved only in a well-defined window of thickness.[22,29,31] The opposite orientation of the PMMA cylinder within the trenches and on the flat area surrounding the gratings indicate that the polymer flow from the mesa into the trenches increases the film thickness in the trenches to such an extent that the perpendicular orientation of the microdomains is not energetically favourable. The second important factor to consider is the presence of the solvent retained inside the polymeric film. This effect is particularly relevant in the case of toluene because of its relatively low volatility. Since the solvent is mainly confined at the substrate surface/polymer interface, the increased interfacial area of the confined polymeric film inside the trenches results in a large amount of retained solvent.[32] In the case of conventional thermal treatment in a furnace/oven the amount of solvent inside the nanometric film is strongly reduced during the long heating ramp necessary to reach the annealing temperature. In contrast, the RTP process involves a very fast heating rate to the final annealing temperature (20 °C s^{-1}) and consequently the solvent desorption during the heating stage is substantially reduced. As a result, a significant amount of solvent is still available inside the film during the isothermal stage of the thermal treatment and can actively participate in the BCP ordering process.[19] During the RTP process, a progressive solvent evaporation occurs which, on one hand, produces a powerful and highly directional field able to promote the perpendicular orientation and, on the other hand, gradually reduces the thickness of the polymeric film (Fig. 7c). The solvent release during the annealing treatment allows the film inside the trenches to reach the critical thickness that promotes the perpendicular arrangement of the microdomains. According to this view, the flipping rate should be higher in the trenches with the lower thickness, that is in the central ones, and should decrease as the thickness increases, that is toward the periphery of the grating, as experimentally observed. Similarly, different flipping velocities are expected depending on the geometrical parameters. Since the BCP thickness inside the individual trenches depends on the quantity of BCP present on the mesa, which acts as a reservoir, a slower flipping kinetics is expected for trenches separated by large mesas, in agreement with the experimental data (Fig. 4b). In addition, a faster

flipping kinetics is observed in the larger trenches, since the polymer flow results in a limited increase of the film thickness (Fig. 4b). The same rearrangement, from a parallel to perpendicular orientation with respect to the substrate, is observed in the case of RCP-functionalized and bare substrates, supporting the idea that a common mechanism drives the flipping process.

The neutralization of the substrate only affects the disposition of the cylinders with respect to the long axis of the trenches. These experimental results demonstrate that RTP treatment exhibits significant similarities with SVA and supports the idea of a fundamental role, in the ordering process, of the solvent, which is naturally retained in the polymeric film during the spinning. This interpretation is perfectly consistent with the very fast ordering we have recently reported for symmetric and asymmetric PS-*b*-PMMA block copolymers on flat substrates when treated in RTP.[19] In this regard the present manuscript corroborates the idea that RTP is not just faster and cheaper than conventional thermal treatments, but it is fundamentally different and more powerful. Further investigations are required to delineate the real potentialities of this experimental approach.

Conclusions

The experimental findings herein reported demonstrate that RTP enables ordering phenomena similar to those observed by SVA but in a much shorter time and without the need for solvent vapor inside the annealing chamber. A fine tuning of the orientation of the asymmetric PS-*b*-PMMA nano-domains is possible when confined in topographically defined structures; flipping of the nanodomains from parallel to perpendicular orientation with respect to the surface is achieved by simply adjusting the annealing time of the process. The possibility to promote the organization of the PMMA cylinder parallel to the substrate with an orientation either normal or parallel with respect to the long axis of the trenches in as few as 30 s is also demonstrated. From a technological point of view, these results suggest that RTP technology offers many fundamental advantages over conventional thermal treatments and can be regarded as a solvent assisted thermal process in which the solvent is the naturally entrapped one in the polymeric film after the spinning process.

Experimental

Trench fabrication

In order to study the evolution of the morphology as a function of the geometrical parameters of the trenches, several groups of trenches having different widths (W) and located at a distance (d) were fabricated. Nanolithography of the trenches was carried out using a FEI Quanta 3D dualbeam SEM-FEG equipped with NPGS by J. C. Nabity on PMMA resists at 30 kV after an accurate exposure dose test with a 6 pA current. Resists were developed in standard MIBK–IPA 1 : 3 solution for 60 s, stopped in IPA for 20 s and rinsed in DI water for 20 s. RIE was performed in a Plasmalab 80 Plus at a pressure of 40 mTorr. The power of the RF generator was set at 120 W and the bias voltage at 340 V. The gas was a mixture of CHF_3 (60 sccm) and Ar (25 sccm). The etching was calibrated and a linear dependence of the etched thickness as a function of time was observed.

Substrate neutralization

Random copolymer P(S-*r*-MMA) with a styrene fraction 0.62, M_n = 13 500 g mol^{-1} and PDI = 1.26 (Polymer Source) was purchased from Polymer Source Inc. and used without further purification. A solution with 18 mg of P(S-*r*-MMA) in 2 ml of toluene was prepared in an ultrasonic bath. The –OH terminations of the random copolymer were used to graft the copolymer to a silicon oxide layer. The solution was spun for 30 seconds at 3000 rpm. In order to induce the grafting process the samples were annealed in the RTP for 60 s. To allow chain ends to diffuse and react with the substrate, the temperature was set at 250 °C, well above the glass transition temperature of the copolymers. The non-anchored chains were removed after the annealing with a 300 s sonication bath in toluene. The thickness of the resulting layer was 8 ± 0.4 nm as detected by ellipsometry measurements. In samples with no RCP neutralization, only the cleaning process was performed on the patterned substrate.

Block copolymer deposition

Asymmetric PS-*b*-PMMA with a styrene fraction of 0.71, M_n = 67 100 and PDI = 1.09 was purchased from Polymer Source Inc. and used without further purification. A solution with PS-*b*-PMMA in toluene was prepared (18 mg in 2 ml). Also in this case the annealing was performed in a N_2 atmosphere at 250 °C. The annealing time was also varied between 10 s and 900 s, in order to promote self-organization into hexagonal arrangements of PMMA cylinders in a PS matrix. The domain period of such cylindrical features is $L_0 \sim 35$ nm. The PS nanotemplate formation was completed by the selective removal of the cylindrical PMMA blocks. A 10 minute exposure to ultraviolet radiation (5 mW cm^{-2}, λ = 253.7 nm) allows degradation of the PMMA and cross-linking of the PS matrix. The PMMA cylinders were removed by immersion in an acetic acid bath and subsequent rinsing in deionized water. Finally oxygen plasma treatments were performed to remove the random copolymer at the bottom of the pores.

Acknowledgements

This research activity was partially funded by the ERANET PLUS "NanoSci-E+" consortium through the NANO-BLOCK project and the EMRP Joint Research Project SiB61 CRYSTAL. Patent protection related to this work is pending.

Notes and references

1 International Technology Roadmap for Semiconductors, 2011 Edition, Emerging Research Materials.
2 R. A. Segalman, B. McCulloch, S. Kirmayer and J. J. Urban, *Macromolecules*, 2009, **42**, 9205–9216.
3 S. B. Darling, *Prog. Polym. Sci.*, 2007, **32**, 1152.

4 L. Persano, A. Camposeo and D. Pisignano, *J. Mater. Chem. C*, 2013, **1**, 7663–7680.
5 Y. S. Jung, J. B. Chang, E. Verploegen, K. K. Berggren and C. A. Ross, *Nano Lett.*, 2010, **10**, 1000.
6 E. Han, H. Kang, C.-C. Liu, P. F. Nealey and P. Gopalan, *Adv. Mater.*, 2010, **22**, 4325.
7 M. P. Stoykovich, M. Muller, S. O. Kim, H. H. Solak, E. W. Edwards, J. J. de Pablo and P. F. Nealey, *Science*, 2005, **308**, 1442.
8 S. J. Jeong, J. E. Kim, H. S. Moon, B. H. Kim, S. M. Kim, J. B. Kim and S. O. Kim, *Nano Lett.*, 2009, **9**, 2300.
9 C. T. Black and O. Bezencenet, *IEEE Trans. Nanotechnol.*, 2004, **3**, 412–415.
10 D. Sundrani, S. B. Darling and S. J. Sibener, *Nano Lett.*, 2004, **4**, 273.
11 J. Y. Cheng, F. Zhang, V. P. Chuang, A. M. Mayes and C. A. Ross, *Nano Lett.*, 2006, **6**, 2099.
12 D. Sundrani, S. B. Darling and S. J. Sibener, *Langmuir*, 2004, **20**, 5091.
13 A. M. Welander, H. Kang, K. O. Stuen, H. H. Solak, M. Muller, J. J. de Pablo and P. F. Nealey, *Macromolecules*, 2008, **41**, 2759.
14 S. Ji, C. C. Liu, W. Liao, A. L. Fenske, G. S. W. Craig and P. F. Nealey, *Macromolecules*, 2011, **44**, 4291.
15 X. Zhang, K. D. Harris, N. L. Y. Wu, J. M. Murphy and J. N. Buriak, *ACS Nano*, 2010, **11**, 7021.
16 G. Kim and M. Libera, *Macromolecules*, 1998, **31**, 2569–2575.
17 X. Zhang, K. D. Harris, N. L. Y. Wu, J. N. Murphy and J. M. Buriak, *ACS Nano*, 2010, **4**, 7021–7029.
18 C. Sinturel, M. Vayer, M. Morris and M. A. Hillmyer, *Macromolecules*, 2013, **46**, 5399–5415.
19 F. Ferrarese Lupi, T. J. Giammaria, M. Ceresoli, G. Seguini, K. Sparnacci, D. Antonioli, V. Gianotti, M. Laus and M. Perego, *Nanotechnology*, 2013, **24**, 315601.
20 J. Y. Cheng, A. M. Mayers and C. A. Ross, *Nat. Mater.*, 2004, **3**, 823–828.
21 M. Perego, A. Andreozzi, A. Vellei, F. Ferrarese Lupi and G. Seguini, *Nanotechnology*, 2013, **24**, 245301.
22 A. Andreozzi, E. Poliani, G. Seguini and M. Perego, *Nanotechnology*, 2011, **22**, 185304.
23 M. Kim, W. Han, D. P. Sweat and P. Gopalan, *Soft Matter*, 2013, **9**, 6135–6141.
24 R. Ruiz, R. L. Sandstorm and C. T. Black, *Adv. Mater.*, 2007, **19**, 587–591.
25 R. Ruiz, N. Ruiz, Y. Zhang, R. L. Sandstorm and C. T. Black, *Adv. Mater.*, 2007, **19**, 2157–2162.
26 P. Mokarian-Tabari, T. W. Collins, J. D. Holmes and M. A. Morris, *ACS Nano*, 2011, **5**, 4617–4623.
27 S. Roy, K. J. Ansari, S. S. K. Jampa, P. Vutukuti and R. Mukherjee, *ACS Appl. Mater. Interfaces*, 2012, **4**, 1887–1896.
28 T. G. Fitzgerald, R. A. Farrell, N. Petkov, C. T. Bolger, T. M. Shaw, J. P. F. Charpin, J. P. Gleeson, J. D. Holmes and M. A. Morris, *Langmuir*, 2009, **25**, 13551–13560.
29 G. Kraush and R. Magerle, Nanostructured Thin Films *via* Self-Assembly of Block Copolymers, *Adv. Mater.*, 2002, **14**, 1579–1583.
30 H.-D. Kon, Y. J. Park, S.-J. Jeong, Y. N. Kwon, I. T. Han and M.-J. Kim, *J. Mater. Chem. C*, 2013, **1**, 4020–4024.
31 I. A. Zucchi, E. Poliani and M. Perego, *Nanotechnology*, 2010, **21**, 185304.
32 J. Garcia-Turiel and B. S. Jerome, *Colloid Polym. Sci.*, 2007, **285**, 1617–1623.